International Forum on Aeroelasticity and Structural Dynamics
IFASD 2024
17-21 June 2024, The Hague, The Netherlands

# THE DESIGN AND ANALYSIS OF TENSEGRITY MORPHING WING

**Jie Yu[1], Song Chen[2], Zhang Haibo[3]**

[1] Beihang university
[2] Beihang university
[3] Beihang university

**Keywords:** Tensegrity System, Morphing Wing, Static Deflection, Aerodynamic Analysis

**Abstract:** Tensegrity systems are the lightweight self-equilibrium structures that compose of a series of tensioned cables and compressed struts. Of particular interest, adjusting the pretension of the tensegrity can tailor the structural characteristics as needed without a basic configuration change. By changing the length of cables or struts, the tensegrity system can morph while maintaining its inherent strength and stiffness. This makes tensegrity systems an attractive candidate for morphing aircraft wings. In addition, due to the influence of external forces on the stiffness matrix, the deflection analysis of the tensegrity wing after being subjected to aerodynamic forces are nonlinear. In this article, based on the aerodynamic shape of the RV-4 wing, we design a feasible tensegrity morphing wing using the R-cross structures. A numerical example is provided to simulate the aerodynamic load and static deflection on this three-dimensional tensegrity morphing wing under different working condition. The results show that our tensegrity morphing wing is 80% of the weight of the RV4 wing， while they have the comparable static deflection with the rudder angle of $10^o$.The deflection of the tensegrity morphing wing is smaller than that of the traditional wing under the condition of the rudder angle of $0^o$. In addition, when the rudder angle has been changed from $0^o$ to $10^o$, the torsion angle variation of the tensegrity morphing wing is also smaller than that of the traditional wing, which is $1.5514^o$ and $20.5714^o$, respectively.

## 1 INTRODUCTION

Tensegrity structure , also called tensegrity systems, is a self-equilibrium structure composed of a series of tensioned cables and compressed struts [1]. It has the advantages of lightweight, reasonable stress, controllable shape, and novel form. Common structural forms are shown in Figure 1. In the 1940s, American architect R B. Fuller invented the tensegrity structure and applied it in the field of architecture [2]. The study of its mechanical properties has been deeply explored, including equilibrium[3], stiffness[4], preloading[5], and stability[6].

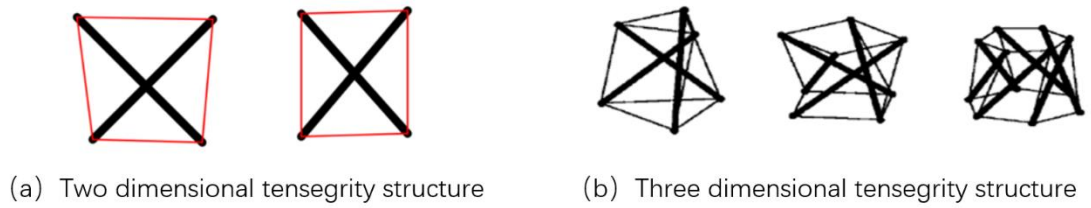


**Figure 1: Common tensioning structures**

The load-carrying structure of aircraft wings mainly consist of stringers, ribs, and spars, which are often made of heavy alloys. With the rapid development of the aviation industry, the performance and quality requirements of aircraft are also increasing. In order to improve the flying performance and fuel efficiency, the lightweight design and optimization of aircraft wings have become an important research direction. The tensegrity structure not only effectively reduces the wing weight due to its lightweight and high-strength characteristics, but also can be used in morphing wing design due to its variable shape[7]. Moreover, the structural stiffness of tensegrity systems is related to pre-tension, which allows the same tensegrity wing design to meet different task requirements by changing the pre-tension to present different wing mechanical properties[8].

The tensegrity structure has many design applications in wings. In terms of underwater biomimetic wings, Kemp et al.[9] studied the pectoral fins of the manta ray and designed a biomimetic wing based on a class II tensegrity structure. Yan[10] further analyzed and studied the internal structural characteristics of the pectoral fins of manta rays, and designed a new biomimetic wing structure using a multi groove motor driven pulley that can adjust the stiffness of the biomimetic fins by changing the tension of the elastic rope in the biomimetic fins. In terms of aircraft wing design, Skelton[8] displayed a concept for a tension wing that has the ability to alter its twin. Chen et al.[11] utilized the tensegrity structure to design a novel two- dimensional morphing airfoil. Myszka et al.[7] quantitatively compared the strength and stiffness of tensegrity structures with some common traditional structures to evaluate their ability as aircraft wings. The results indicate that the tensegrity structures have high strength and equivalent stiffness under all loads, and the R-cross structure performs the best among all the tensegrity structures. On the basis of Myszka's research, Mills et al.[12] proposed a tensegrity wing and its topology-optimized wing based on R-cross structure, and compared them with traditional wing. The results show that, under the condition of equivalent deflection and strain energy, the weight of a tensegrity wing is 59% of the traditional wing, while the weight of a topology-optimized tensegrity wing is 49% of the traditional wing. This greatly reduces the weight of the wing and provides a new research approach for the development of aircraft wings towards lightweight and morphing capacity. It is worth mentioning that the wing is a fixed structure and has no maneuverability.

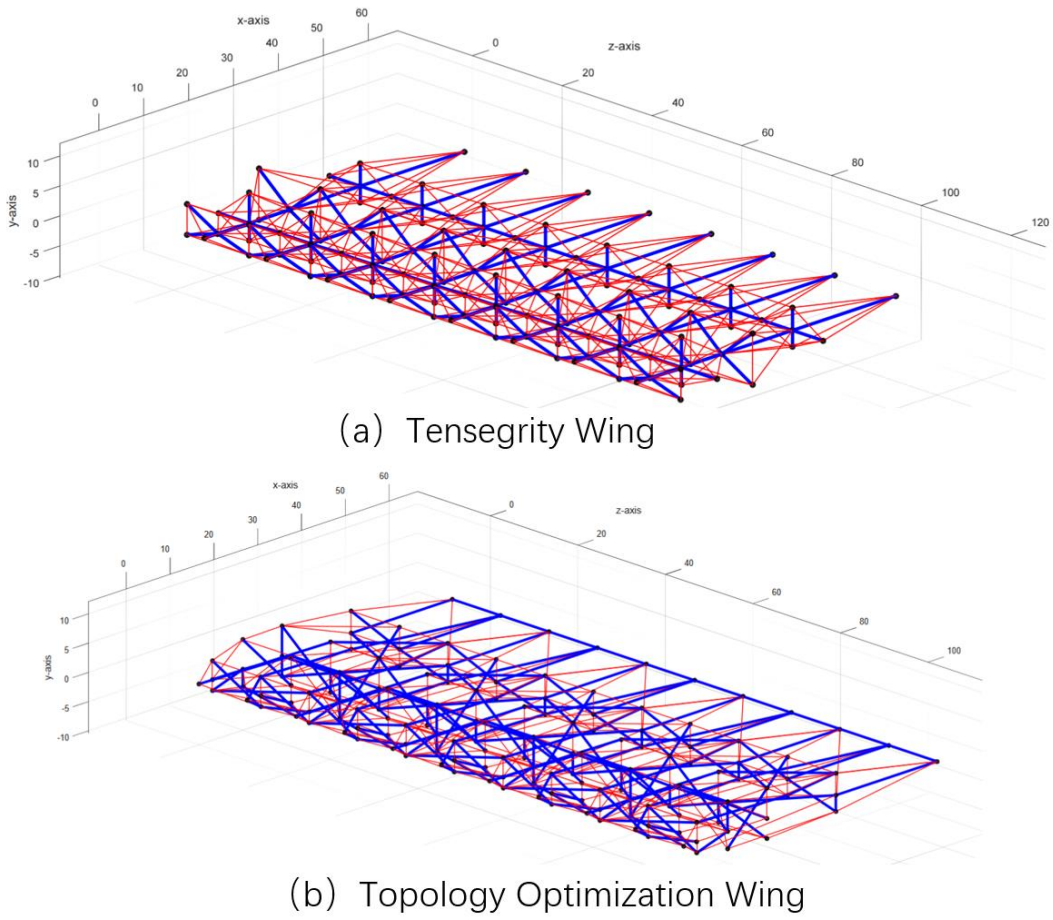


**Figure 2: Tensegrity wing and its topology optimization proposed by Mills**[12]

This article is based on the research of Mills[12] and proposes a morphing scheme for tensegrity wings to obtain control ability in flight. The tensegrity morphing wing is compared with traditional wings under certain static aerodynamic conditions. The second part introduces the basic theory of tensegrity systems. The third part introduces the design scheme of tensegrity morphing wings. The fourth part shows the aerodynamic response of tensegrity morphing wing and traditional wing under two operating conditions of rudder angles of $0^o$ and $10^o$.

## 2 TENSEGRITY

### 2.1 Geometry

A general tensegrity structure is composed of $n$ nodes joined by $m$ members. Number nodes from small to large. the coordinates of node $i$ are represented by vector $\boldsymbol{n_i} = \{x_i, y_i, z_i\}^T$, and the system node matrix is defined as

$$\boldsymbol{N}=[\boldsymbol{n_1},\boldsymbol{n_2},...,\boldsymbol{n_n}]=\begin{bmatrix} x_1,x_2,...,x_n \\ y_1,y_2,...,y_n \\ z_1,z_2,...,z_n \end{bmatrix}=\begin{bmatrix} \boldsymbol{x} \\ \boldsymbol{y} \\ \boldsymbol{z} \end{bmatrix},\in \mathbb{R}^{3\times n} \tag{1.1}$$

For the member $k$, which connects node $i$ to node $j$, the $(k,p)$ element in the connectivity matrix $\boldsymbol{C}$ is

$$C_{(k,p)}=\begin{cases} 1,\text{if p=j} \\ -1,\text{if p=i} \\ 0,\text{otherwise} \end{cases},p=1,2,...,n \tag{1.2}$$

The projection $u$、$v$、$w$ of the direction vectors of each component in the $x$、$y$、$z$ directions are

$$\begin{cases} \boldsymbol{u}=\boldsymbol{Cx} \\ \boldsymbol{v}=\boldsymbol{Cy} \\ \boldsymbol{w}=\boldsymbol{Cz} \end{cases},\in \mathbb{R}^{m\times 1} \tag{1.3}$$

The length of member $k$ is $l_k=\sqrt{u_k^2+v_k^2+w_k^2}$. To improve computational efficiency, diagonalize vectors

$$\begin{aligned} \boldsymbol{U}=diag(\boldsymbol{u}) \quad \boldsymbol{V}=diag(\boldsymbol{v}) \\ \boldsymbol{W}=diag(\boldsymbol{w}) \quad \boldsymbol{L}=diag(\boldsymbol{l}) \end{aligned} \tag{1.4}$$

## 2.2 Equilibrium ,Pre-Tension and Force-density Matrix

The cables must be kept in tension $(t>0)$ and the struts in pressure $(t<0)$ during the stressing of the tensegrity structure. The internal forces of members are represented by vectors $\boldsymbol{t}$, and the initial pre-tension is defined as $\boldsymbol{t_0}$. The external force applied to node $i$ is represented by a vector $\boldsymbol{f}_i=\{f_{ix},f_{iy},f_{iz}\}^T$, and the system external force matrix is $\boldsymbol{F}=[\boldsymbol{f_1},\boldsymbol{f_2},...,\boldsymbol{f_n}]^T\in\mathbb{R}^{3\times n}$. The external force vector is $\boldsymbol{f}=vec(\boldsymbol{F})\in\mathbb{R}^{3n\times 1}$.

The equilibrium equation for the tensegrity structure is[13]

$$\boldsymbol{At}=\boldsymbol{f} \tag{1.5}$$

Among them, $\boldsymbol{A}$ is the equilibrium matrix. When the external force is 0, the initial pre-tension solution equation can be obtained as

$$\boldsymbol{At^0}=\boldsymbol{0} \tag{1.6}$$

According to matrix factorization theory, there exists unitary matrix $\boldsymbol{R} \in \mathbb{R}^{3n\times 3n}$ , $\boldsymbol{T} \in \mathbb{R}^{m\times m}$ satisfies the equation[14]

$$\boldsymbol{A} = \boldsymbol{R}\begin{pmatrix} \boldsymbol{S} & \boldsymbol{0} \\ \boldsymbol{0} & \boldsymbol{0} \end{pmatrix}\boldsymbol{T} \tag{1.7}$$

$\boldsymbol{R}$、$\boldsymbol{T}$ are orthogonal matrix. Let $r = rank(\boldsymbol{A})$, $\boldsymbol{R} = [\boldsymbol{R_r}, \boldsymbol{R_p}]$, $\boldsymbol{T} = [\boldsymbol{T_r}, \boldsymbol{T_s}]$ ,where $\boldsymbol{R_p}$ is the orthogonal product of the node displacement space, known as the mechanism displacement mode; $\boldsymbol{T_s}$ is orthogonal product of the internal force space of the element, and is the self-tension mode; $p = 3\times n - r$ and $s = m - r$ are the mechanism displacement mode number and self-tension mode number. The possible mechanical displacement of nodes $\boldsymbol{d_p}$ and the possible pre-tension of structures $\boldsymbol{t_{pre}}$ can be represented by:

$$\begin{aligned} \boldsymbol{d}_p &= \boldsymbol{R}_p\boldsymbol{\alpha} \\ \boldsymbol{t}_{pre} &= \boldsymbol{T}_s\boldsymbol{\beta} \end{aligned} \tag{1.8}$$

where $\boldsymbol{\alpha}$、$\boldsymbol{\beta}$ are any column vector. It is worth mentioning that the mechanism displacement mode and self-tension mode also satisfy the following conditions:

$$\begin{aligned} \boldsymbol{A}^T\boldsymbol{d}_p &= \boldsymbol{A}^T\boldsymbol{R}_p = 0 \\ \boldsymbol{A}\boldsymbol{t}_{pre} &= \boldsymbol{A}\boldsymbol{T}_s = 0 \end{aligned} \tag{1.9}$$

The internal force density of member $k$ is $q_k = t_k / l_k$ , and the force density vector is $\boldsymbol{q} = [q_1, q_2, ..., q_m]$.The force density matrix of tensegrity structure is constructed

$$\boldsymbol{E} = \boldsymbol{C}^T\boldsymbol{Q}\boldsymbol{C} \tag{1.10}$$

where the matrix $\boldsymbol{Q} = diag(\boldsymbol{q})$. In addition, the force density matrix can be also directly obtained from the force density of the member. The $(i,j)$th entry $E_{(i,j)}$ of the force density matrix $\boldsymbol{E}$ is defined as:

$$\boldsymbol{E}_{(i,j)} = \begin{cases} \sum_{k\in K_i} q_k\,, & if\ i = j \\ -q_k, & if\ nodes\ i\ and\ j\ are\ connected\ by\ member\ k \\ 0, & \text{other cases} \end{cases}$$

where $K_i$ is the set of members connected to node $i$.

### 2.3 Stiffness and Deflection

The stiffness matrix $\boldsymbol{K}$ of the tensegrity structure consists of an elastic stiffness matrix $\boldsymbol{K_E}$ and a geometric stiffness matrix $\boldsymbol{K_G}$[15]:

$$\boldsymbol{K} = \boldsymbol{K_E} + \boldsymbol{K_G} \tag{1.11}$$

$$\boldsymbol{K_E} = \boldsymbol{A}\bar{\boldsymbol{K}}\boldsymbol{A}^{\boldsymbol{T}} \tag{1.12}$$

$$\boldsymbol{K_G} = \boldsymbol{I_3} \otimes \boldsymbol{E} \tag{1.13}$$

where $\bar{\boldsymbol{K}} = diag(E_1A_1/l_1, E_2A_2/l_2, ..., E_mA_m/l_m)$, $E_kA_k$ is the tensile and compressive stiffness of member $k$, $\boldsymbol{I_3}$ is a $3 \times 3$ identity matrix, $\otimes$ is the tensor product. Define the node deflection as $\boldsymbol{d} = \{d_{1x}, ..., d_{nx}, d_{1y}, ..., d_{ny}, d_{1z}, ..., d_{nz}\}^T \in \mathbb{R}^{3n\times 1}$. Then,

$$\boldsymbol{Kd} = \boldsymbol{f} \tag{1.14}$$

The relationship between node deflection $\boldsymbol{d}$ and member elongation $\boldsymbol{e}$ is

$$\boldsymbol{A^T d} = \boldsymbol{e} \tag{1.15}$$

The change in member stress is

$$\boldsymbol{\sigma} = \bar{\boldsymbol{K}}\boldsymbol{e} \tag{1.16}$$

Note that the stiffness matrix $\boldsymbol{K}$ of the tensegrity structure is related to the initial pre-tension, and when an external force acts on the nodes, the displacement of the node causes a change in the force density matrix, resulting in changes in the stiffness matrix. Therefore, the solution of the above equation is nonlinear. The usual solution method is to use a small incremental gradual force application method to ensure the equilibrium of the structure and update the stiffness matrix. Maintain the positive definite of the stiffness matrix $\boldsymbol{K}$ at all times during the solving process to ensure the stability of the structure.

## 3 TENSEGRITY MORPHING WING

### 3.1 R-cross structure and force-finding

The composition of the R-cross structure is shown in Figure 3. This structure consists of 6 struts (marked as $m_1$ to $m_6$) and 12 cables (marked as $m_7$ to $m_{18}$) connected at 7 nodes (marked as $n_1$ to $n_7$). The number of mechanism displacement modes and self-tension modes are $p = 6$ and $s = 3$.

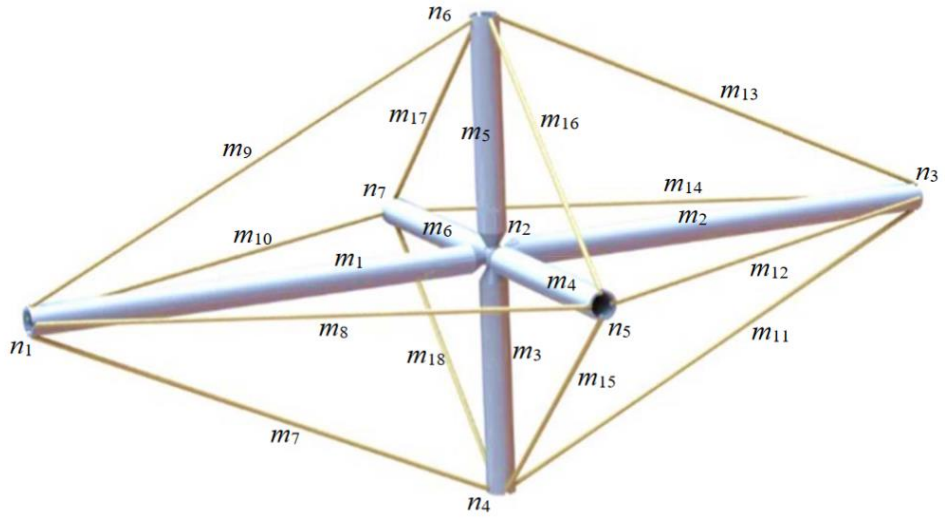


**Figure 3: R-cross structure**[12]

In the design of a tensegrity structure, the process of determining its geometric shape and initial pre tension is called Form Finding. In specific form finding methods, the main variables can be shape parameters or internal force parameters. Therefore, according to the different main variables used, form finding methods can be divided into two categories: "shape finding" and "force finding". The representative algorithms of the former include the well-known dynamic relaxation method[16,17], force density method[18], and energy method[19], while the latter mainly appears as the search for feasible pre-stress or pre-stress optimization algorithm[20–24]. This article is based on the content of the second part, using genetic algorithm to search and optimize feasible pre-tension.

According to formula(1.8), the feasible pre-tension can be obtained by linearly combining the self-tension modes, so different pre-tension can be obtained by using vectors $\boldsymbol{\beta}$ as optimization variables. In general, the force finding focuses more on whether the obtained pre-tension meets the constraint conditions, namely compression struts and tension cables, and does not put forward too many requirements for the optimization objective, which is generally set as $\min(\|\boldsymbol{\beta}\|_2)$. This optimization objective has good universality when there is no actual optimization object or design purpose, but for the convenience of saving raw materials and future production, we hope that the internal forces of the members are as uniform as possible. Therefore, we use the root mean square of absolute deviation to measure the uniformity of internal forces:

$$h(\boldsymbol{\beta}) = \frac{\sqrt{\sum_{i=1}^{m}(|t_i| - \bar{t})^2}}{\bar{t}} \tag{2.1}$$

where $\bar{t} = \frac{\|\boldsymbol{t}_{pre}\|_2}{m}$. So the optimization objective function is

$$F(\boldsymbol{\beta}) = \| \boldsymbol{\beta} \|_2 + h(\boldsymbol{\beta}) \tag{2.2}$$

Let the first 6 members as compression struts and the last 12 members as tension cables, with a feasible pre-stress of $\boldsymbol{t}_{pre} = [t_1, t_2, ..., t_{18}]$. The optimization problem corresponding to the process of force finding is

$$\begin{cases} \min(F(\boldsymbol{\beta})) \\ s.t. \ \ \beta_i \in [-1,1] \\ t_i < 0, i = 1,2,...,6 \\ t_j > 0, \ j = 7,8,...,18 \end{cases} \tag{2.3}$$

### 3.2 Tensegrity Morphing Wing Design

The Van's RV-4[25], a manned aircraft produced by Van's Aircraft and sold as a kit, was selected as the baseline aircraft for the presentation structural comparison study Its wing, referred to as the traditional wing in the lower part, has a NACA23015 airfoil, with a single wing weight of 25.7kg (with skin) and 10.08kg (without skin), a chord length of 1.47m, and a wingspan of 2.82m. The internal load-bearing structure of the wing is shown in Figure 4.

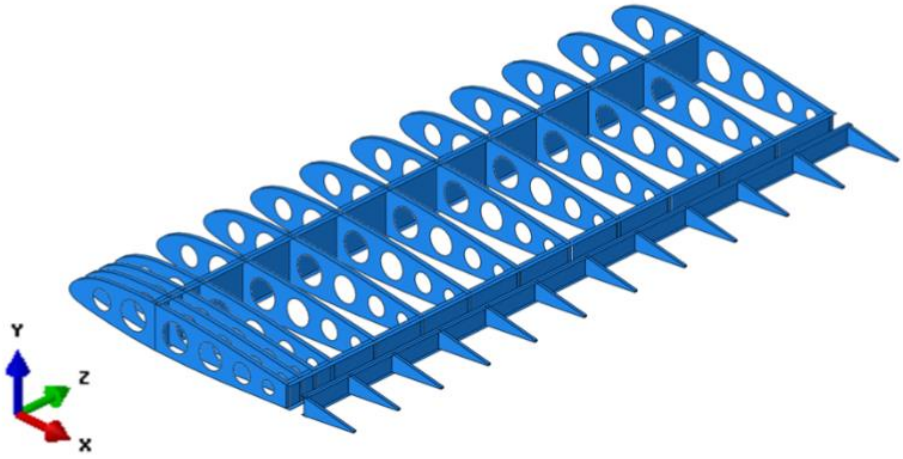


**Figure 4: The conventional wing structure** [12,26]

The tensegrity wing is composed of 32 R-cross structures, with 4 R-cross forming a chord element and 8 chord elements distributed along the spanwise direction to form the wing. Each chord element has a spanwise length of 350mm. The first step in wing design is to optimize and determine the positions of the 10 nodes connecting the R-cross with the skin. The optimization goal is to minimize the distance between the segmented curve defined by the nodes and the airfoil. The optimized positions of 8 nodes with leading and trailing edge points are shown in Figure 5 and Table 1, and the four types of R-cross and chord element are shown in Figure 6.

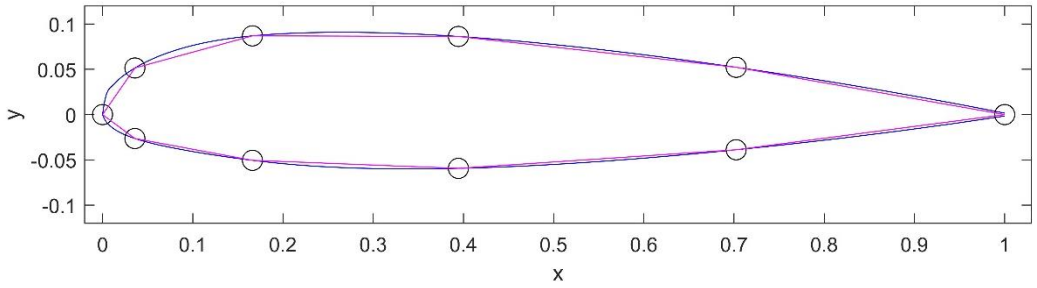


**Figure 5: The optimal locations for 10 nodes to approximate a NACA 23015 airfoil**

**Table 1: Coordinates of the 8 optimal nodes**

| $x$ | 0.035839 | 0.166137 | 0.394436 | 0.702366 |
|---|---|---|---|---|
| $y$/Upper Wing Surface | 0.051459 | 0.086919 | 0.086253 | 0.052217 |
| $y$/ Lower Wing Surface | -0.026419 | -0.050502 | -0.059363 | -0.038826 |

The final tensegrity wing designed based on the above optimization results is shown in Figure 7. The compression strut is composed of aluminum tubing, with an elastic modulus of 72GPa, a density of 2700kg/m$^3$, an outer diameter of 11.1mm, and a wall thickness of 1.8mm. The tension cable is made of T700 carbon fiber, with an elastic modulus of 240GPa and a density of 1600kg/m$^3$. Most cables have a radius of 1mm, and some cables are reasonably thickened considering their load-bearing capacity. The specific quantity and radius are shown in Table 2. The wing doesn't have currently morphing capability, with the overall weight of 6.23kg.

**Table 2: Cable radius and quantity**

| Cable Rad(mm) | 1.00 | 1.25 | 1.75 | 2.25 | 2.50 | 2.75 | 3.00 |
|---|---|---|---|---|---|---|---|
| No of Cables | 215 | 89 | 42 | 31 | 11 | 7 | 3 |

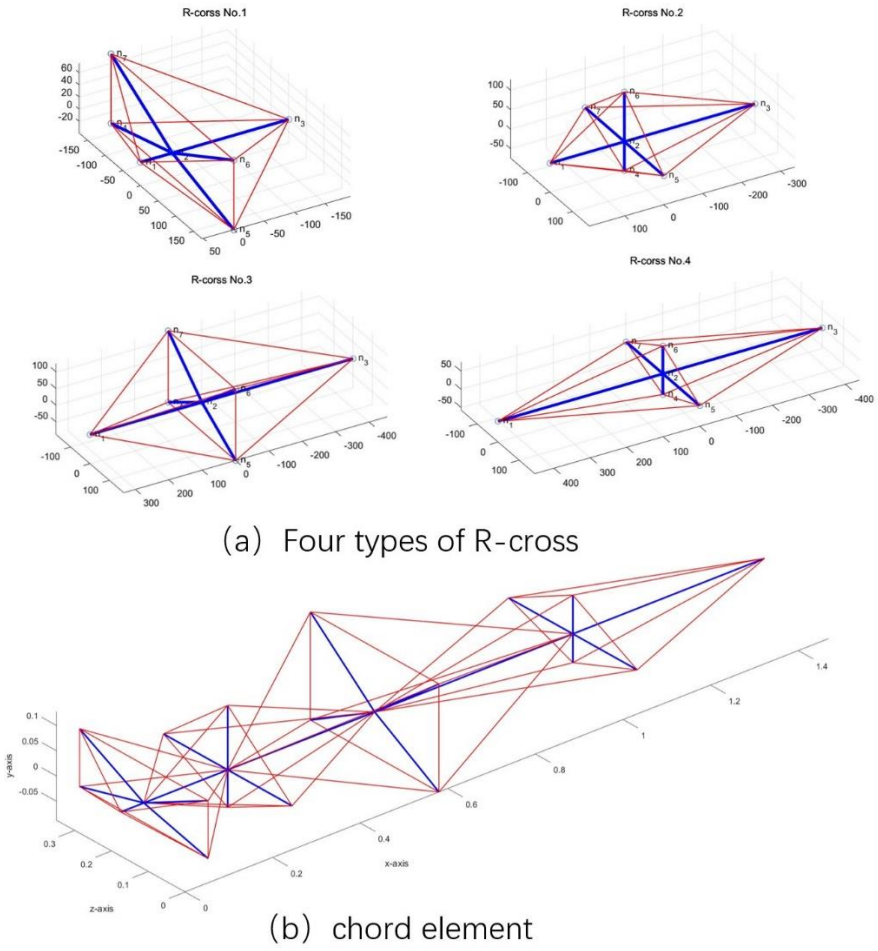


**Figure 6: Four types of R-cross based on optimal nodes and chord element**

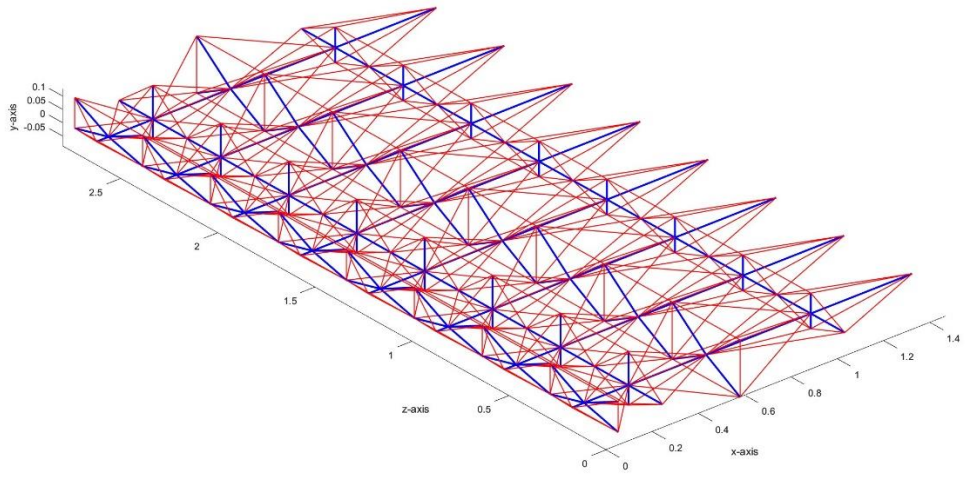


**Figure 7: The tensegrity wing**

Based on the ReCTeR robot being developed by NASA Ames Research Center[27], we have designed an actuator as shown in Figure 8. In order to achieve the morphing capability, we replaced the internal structure of the R-cross. The specific design scheme is to replace the two cables with actuators to achieve structural deformation. The actuator and deformation scheme are shown in Figure 8-Figure **10**. The total weight of a single actuator is approximately 0.12kg, and the weight of the tensegrity morphing wing is 8.15kg.

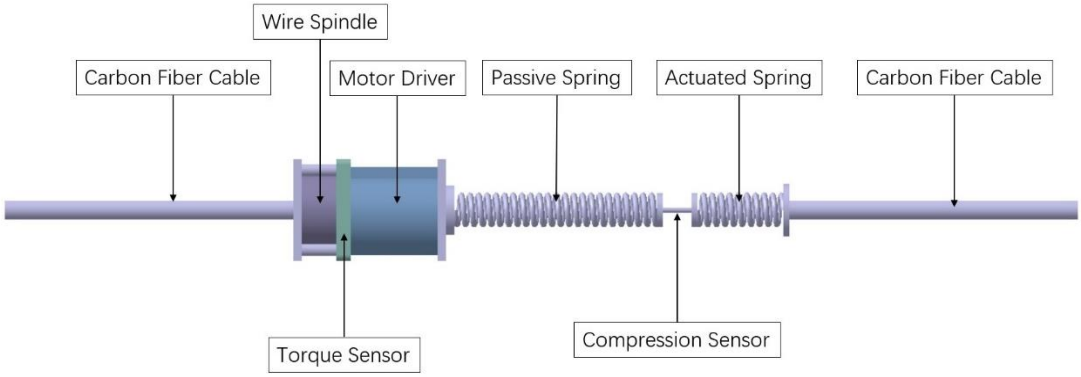


**Figure 8: Actuator concept**

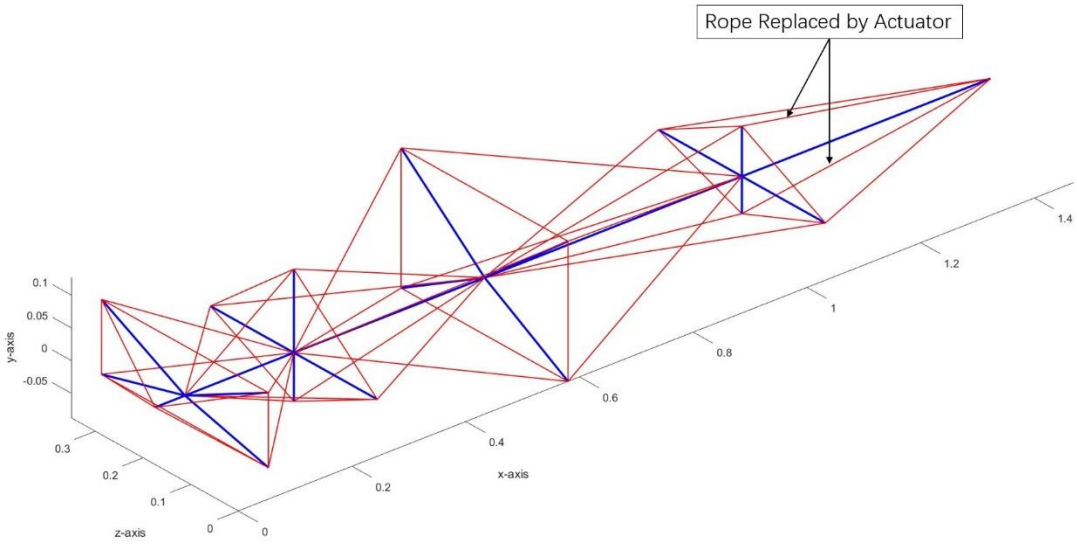


**Figure 9: Actuator location**

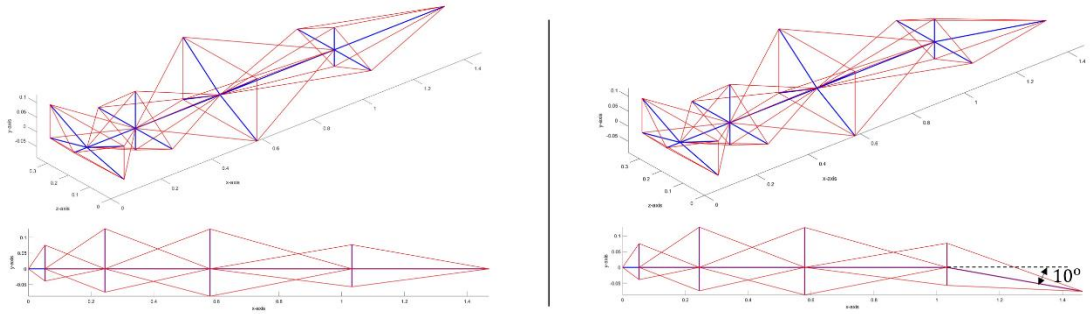


**Figure 10: Deformation of chordal element**

## 4 RESULT AND DISCUSSION

The aerodynamic load condition is selected as a maneuvering speed of 71m/s, with the attack angle of $5^{o}$, using standard atmospheric conditions at sea level. Solve the deflection of traditional wings using Nastran's SOL144 when the ailerons and flaps are deflected downwards by $0^{o}$ and $10^{o}$ respectively.

Analyze the tensegrity wings of the fourth R-cross structure with $0^{o}$ and $10^{o}$ deformations under the same aerodynamic conditions. The analysis method is to first use Fluent to calculate the dynamic and static pressure distribution on the three-dimensional wing surface, then convert it into aerodynamic force distribution, and finally interpolate it into the internal structure of the wing according to a certain proportion distribution to analyze the response of the tensegrity morphing wing. The specific interpolation method is shown in Figure 11. The aerodynamic pressure distribution of wings under different deformation conditions is shown in Figure 12.

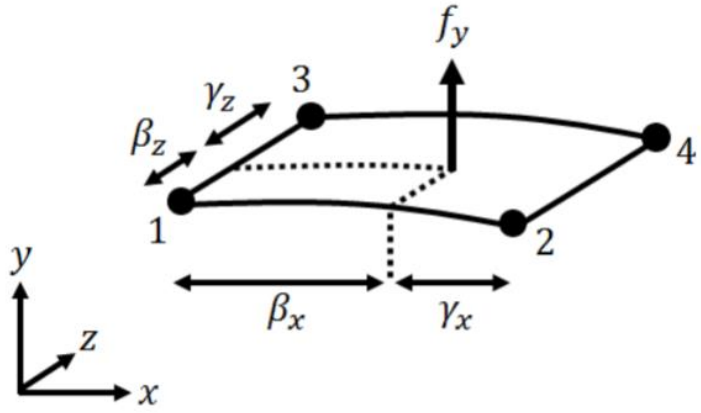


**Figure 11: A diagram showing an aerodynamic force element $f_y$ in the y-direction, at an arbitrary location on the wing surface, and the four closest internal structural nodes, labeled 1, 2, 3, and 4. The dimensions $\beta_z$ and $\gamma_z$ are measured along the z-direction, and the dimensions $\beta_x$ and $\gamma_x$ are measured along the x-direction**[12].

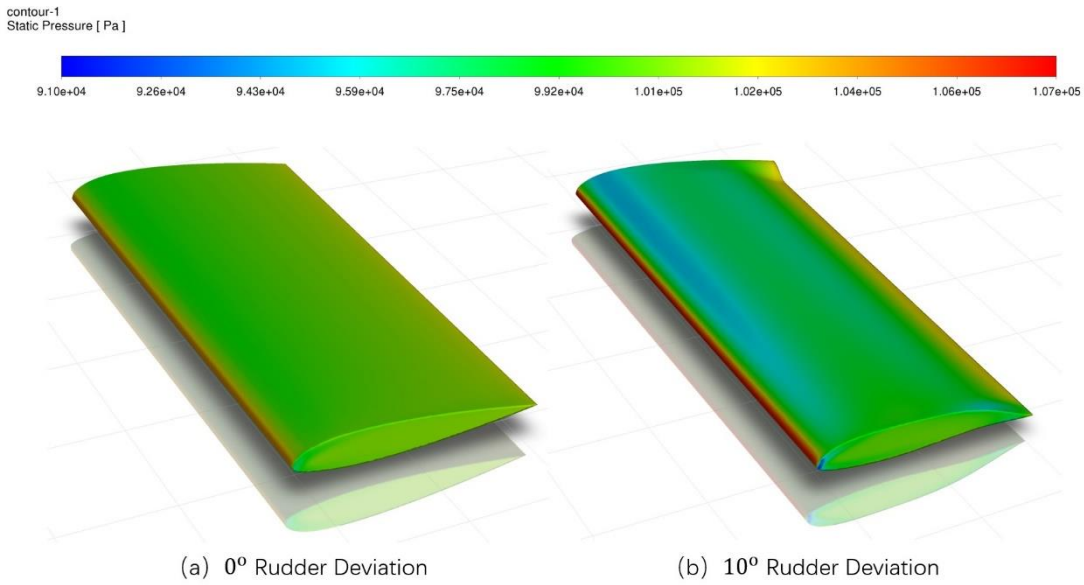


**Figure 12: Static pressure distribution under different working conditions**

The final results are shown in Table 3 and Figure 13-Figure **14**. It can be observed that under the condition of 10° rudder angle, the tensegrity morphing wing can approximately match the maximum deflection of a traditional wing with the same rudder angle at a lower mass, and the maximum deflection caused by the transition of the two conditions is approximate. It is worth mentioning that after the rudder angle changes from 0° to 10°, the traditional wing exhibits a larger torsion angle, while the torsion angle of the tensegrity morphing wing is smaller.

**Table 3: Structural comparison of the conventional wing and tensegrity morphing wing**

| Rudder Angle | | Conventional | Tensegrity |
|---|---|---|---|
| 0° | Leading Edge Deflection | -0.0868 m | 0.0236 m |
| | Trailing Edge Deflection | 0.0485 m | 0.0190 m |
| 10° | Leading Edge Deflection | -0.2457 m | 0.2032 m |
| | Trailing Edge Deflection | -0.3448 m | 0.2384 m |
| 0° to 10° | Max Deflection | 0.2962 m | 0.2194 m |
| | Torsion angle variation | 20.5714° | 1.5514° |

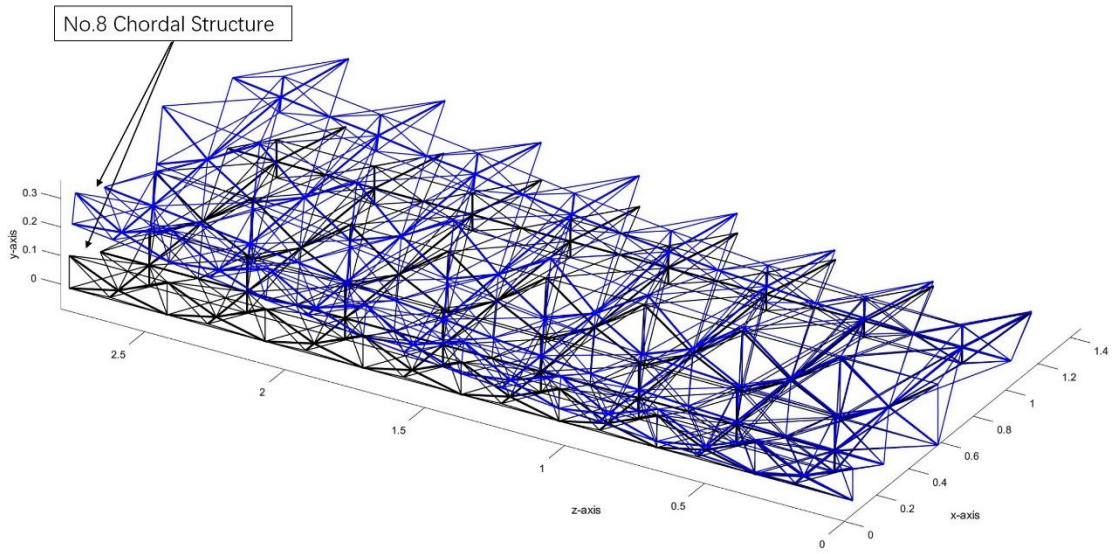


**Figure 13: The deflection of the tensegrity morphing wing with a rudder deviation of $10^{o}$. The black wing is in the unloaded state, while the blue wing is in the loaded state**

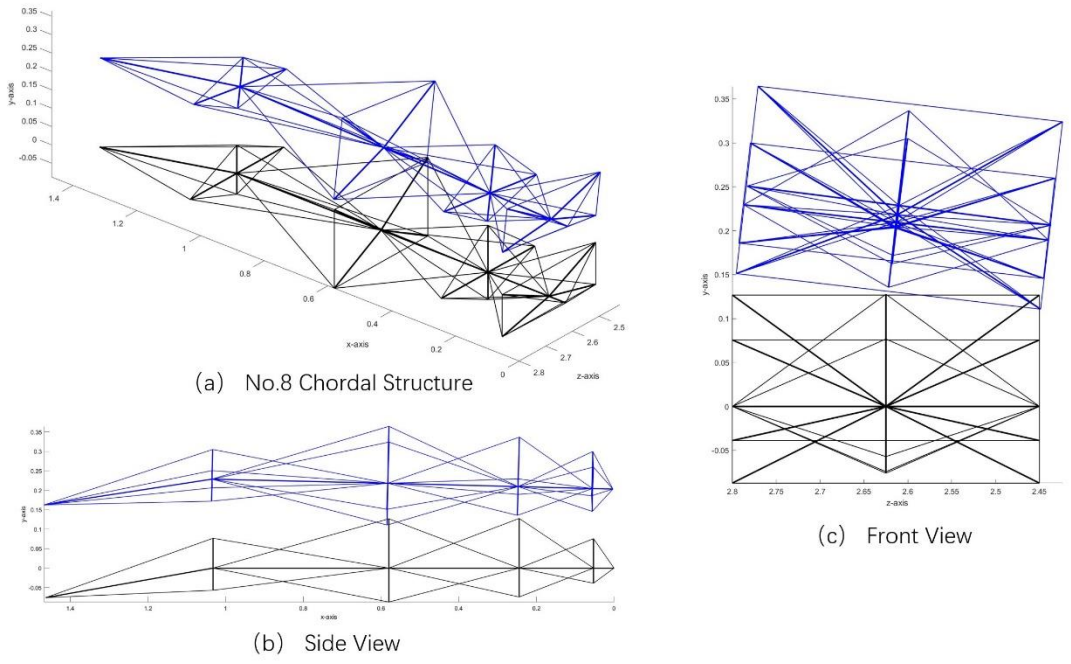


**Figure 14: The deflection of No.8 chordal structure with a rudder deviation of $10^{o}$. The black wing is in the unloaded state, while the blue wing is in the loaded state**

## 5 CONCLUSIONS

This article provides a conceptual scheme for wing with a variable curvature trailing edge designed using the tensegrity structures, which can reduce the structural weight by about 20% compared to the traditional wing design scheme. The static deflection of the tensegrity morphing

wing and the traditional wing under typical operating conditions was compared through numerical examples. The final result shows that the static deflection of the tensegrity morphing wing caused by the aerodynamic force of the $10^{o}$ is equivalent to that of the traditional wing, while the static deflection caused by the aerodynamic force of the $0^{o}$ is smaller than that of the traditional wing. And its torsion angle variation is also smaller than that of the traditional wing.

## REFERENCES


[1] Motro R 2003 Tensegrity : structural systems for the future *E-STREAMS: Electronic reviews of Science and Technology*

[2] Zung T T K and Fuller B 2001 Buckminster Fuller *macmillan*

[3] Williamson D, Skelton R E and Han J 2003 Equilibrium conditions of a tensegrity structure *International Journal of Solids and Structures* **40** 6347–67

[4] Guest S 2005 The stiffness of prestressed frameworks: A unifying approach *International Journal of Solids and Structures* **43** 842–54

[5] Gan L, Yu H, ming T S, Ma weibin and long H H 2021 Analysis of deformation control mechanism of prestressed anchor on jointed soft rock in large cross-section tunnel *Bulletin of Engineering Geology and the Environment* **80** 9089–103

[6] Zhang J Y and Ohsaki M 2006 Stability conditions for tensegrity structures *International Journal of Solids and Structures* **44** 3875–86

[7] Myszka D H and Joo J J 2018 A Study on the Structural Suitability of Tensegrity Structures to Serve As Morphing Aircraft Wings *Volume 5B: 42nd Mechanisms and Robotics Conference* ASME 2018 International Design Engineering Technical Conferences and Computers and Information in Engineering Conference (Quebec City, Quebec, Canada: American Society of Mechanical Engineers) p V05BT07A005

[8] Skelton R E and Oliveira M C D 2009 *Tensegrity Systems* (Tensegrity Systems)

[9] Kemp T H, Kemp T H, Bart-Smith H, Haj-Hariri H, Garner G T, Blemker S S, Dong H and Aylor J H 2018 investigating batoid-inspired propulsion: the development, testing, and performance analysis of a tensegrity-based robotic fin for underwater locomotion

[10] Yan C 2021 *Tensegrity-based biologically-inspired wing design with application in underwater gliders* Master (Tianjin University)

[11] Chen M, Liu J and Skelton R E 2020 Design and control of tensegrity morphing airfoils *Mechanics Research Communications* **103** 103480

[12] Mills A S, Myszka D H, Woods D C, Joo J J and Murray A P 2020 The Structural Suitability of Tensegrity Aircraft Wings *AIAA Scitech 2020 Forum* AIAA Scitech 2020 Forum (Orlando, FL: American Institute of Aeronautics and Astronautics)

[13] Zhang J Y and Ohsaki M 2015 *Tensegrity Structures: Form, Stability, and Symmetry* (Tokyo: Springer Japan)

[14] Connelly R and Back A 1998 Mathematics and Tensegrity *American Scientist* **86** 142

[15] Connelly R and Terrell M 1995 Tenségrités symétriques globalement rigides *Topologie Structurale* **21**

[16] Motro R 1984 Forms and Forces in Tensegrity Systems

[17] Pasquier R Recherche de forme des structures en tenségrité *General Information*

[18] Linkwitz K and Schek H-J 1971 Einige Bemerkungen zur Berechnung von vorgespannten Seilnetzkonstruktionen **40** 145–58

[19] Connelly R R 1993 In Handbook of Convex Geometry

[20] Yuan X F and Dong S U 2002 Nonlinear analysis and optimum design of cable domes *Engineering Structures* **24** 965–77

[21] Masic M and Skelton R E 2006 Selection of prestress for optimal dynamic/control performance of tensegrity structures *International Journal of Solids and Structures* **43** 2110–25

[22] El-Lishani S, Nooshin H and Disney P 2005 Investigating the Statical Stability of Pin-jointed Structures Using Genetic Algorithm *International Journal of Space Structures* **20** 53–68

[23] Lee S, Lee J and Kang J 2017 A Genetic Algorithm Based Form-finding of Tensegrity Structures with Multiple Self-stress States *Journal of Asian Architecture and Building Engineering* **16** 155–62

[24] Trinh D T N, Lee S, Kang J and Lee J 2022 Force density-informed neural network for prestress design of tensegrity structures with multiple self-stress modes *European Journal of Mechanics - A/Solids* **94** 104584

[25] Walker D and Liu D 2015 Topology Optimization of an Aircraft Wing *56th AIAA/ASCE/AHS/ASC Structures, Structural Dynamics, and Materials Conference*

[26] Van's Aircraft Inc 2005 *"RV-4 Construction Manual" RV-4 Preview Plans* (Aurora, Oregon)

[27] Bruce J, Caluwaerts K, Iscen A, Sabelhaus A P and SunSpiral V 2014 Design and evolution of a modular tensegrity robot platform *2014 IEEE International Conference on Robotics and Automation (ICRA)* 2014 IEEE International Conference on Robotics and Automation (ICRA) (Hong Kong, China: IEEE) pp 3483–9

## COPYRIGHT STATEMENT